Available online at www.sciencedirect.com
ScienceDirect
Applied Surface Science 254 (2008) 4632–4637
applied surface science
www.elsevier.com/locate/apsusc

Correlation between optical characterization of the plasma in reactive magnetron sputtering deposition of Zr–N on SS 316L and surface and mechanical properties of the deposited films

A. Fragiel [a,1], R. Machorro [a], J. Muñoz-Saldaña [b], J. Salinas [c], L. Cota [a,*]

[a] *Centro de Ciencias de la Materia Condensada, Universidad Nacional Autónoma de México, Apdo. Postal 2681, C.P. 22800, Ensenada, Baja California, Mexico*

[b] *Centro de Investigación y de Estudios Avanzados del IPN, Unidad Querétaro, Libr. Norponiente No. 2000, Fracc. Real de Juriquilla, 76230 Querétaro, Qro., Mexico*

[c] *Instituto Nacional de Astrofísica Óptica y Electrónica, Apdo Postal 51 y 216, 72000 Puebla, Pue., Mexico*

Received 2 June 2007; accepted 16 January 2008
Available online 31 January 2008

Abstract

Optical and surface spectroscopies as well as nanoindentation techniques have been used to study ZrN coatings on 316L stainless steel obtained by DC-reactive magnetron sputtering. The deposit process was carried out using initial and working pressures of 10^{-6} Torr and 10^{-3} Torr, respectively. The experimental set-up for optical spectra acquisition was designed for the study in situ of the plasma in the deposition chamber. Auger spectroscopy, SEM and X-ray diffraction were used to characterize the coatings. Nanoindentation tests were carried out to measure the mechanical properties of the coating. Plasma characterization revealed the presence of CN molecules and Cr ions in the plasma. Surface spectroscopy results showed that ZrN, Zr_3N_4 and ZrC coexist in the coating. These results allowed the understanding of the mechanical behavior of the coatings, demonstrating the importance of the plasma characterization as a tool for tailoring the properties of hard coatings.

PACS : 62; 68.37.−d; 300.2140; 310.3840

Keywords: Plasma diagnostics; Auger spectroscopy; Nanoindentation; Thin films; Mechanical properties

1. Introduction

Metal nitrides are well known for their characteristic wear and corrosion resistance and high melting point that render them attractive for applications as hard coatings for the tool and decorative industries [1,2]. Different metal nitrides such as TiN, CrN, TaN have been widely studied for particular applications. For instance, ZrN is an attractive material for applications on tool steels, corrosion protection, cryogenic thermometers, integrated circuits, etc. [3–5]. ZrN coatings can be produced by different techniques such as chemical vapor deposition (CVD), physical vapor deposition (PVD) (magnetron sputtering), vacuum arc deposition, pulsed laser deposition, etc. [5,6]. Reactive magnetron sputtering (RMS) has been shown to be a good technique to produce Zr–N coatings, since ion bombardment is known to modify the structure of the substrate, improving the film properties [3]. In the assisted plasma deposition techniques, the final properties of the film may be related to characteristics of the plasma. The study and characterization of the plasma allows the establishment of the conditions for tailoring the properties of hard coatings.

This study is intended to yield information regarding the deposition process to relate the characteristics of the plasma obtained with the morphological, chemical composition and mechanical properties of Zr–N coating formed by reactive unbalanced magnetron sputtering. To do this, optical spectroscopy was applied to analyze the plasma generated during the sputtering deposition process. This is an in situ, not invasive, non-destructive and relatively economic tool to understand and optimize the deposition process.

* Corresponding author. Tel.: +52 646 174 4602; fax: +52 646 174 4603.
E-mail address: leonel@ccmc.unam.mx (L. Cota).
[1] Present address: Instituto de Ingeniería-Ministerio de Ciencia y Tecnología, Caracas, Venezuela.

0169-4332/$ – see front matter © 2008 Elsevier B.V. All rights reserved.
doi:10.1016/j.apsusc.2008.01.104

2. Experimental

Unbalanced magnetron sputtering was used to obtain ZrN coatings on stainless steel 316L. A 99% purity Zr disc was used as target. A combination of mechanical and turbomolecular pumps were used to evacuate the chamber to 10^{-6} Torr. Thereafter, N_2 gas was introduced through a leak valve to obtain a pressure in the 10^{-4} Torr range. The working pressure was in the 10^{-3} range. Prior to the deposition process, the steel substrates were prepared by conventional metallographic polishing and cleaned with acetone and isopropyl alcohol. The substrate temperature during the deposition process was kept between 200 °C and 220 °C.

For the plasma analysis the experimental set-up for optical spectroscopy is shown in Fig. 1. Using a window port on the vacuum chamber, a lens array forms the image of the plasma onto an optical fiber array. Further details of this set-up have been reported elsewhere [8].

The optical fibers were well aligned and coupled to the spectrometer. This set-up allows simultaneous mapping with several fibers of several regions of the plasma. Each fiber records the spectral information corresponding to a particular region of the plasma [8–10]. Thus, the uniformity of the plasma and its spatial variations between the target and substrate space can be traced. For simplicity, only three regions are reported here, one near the target (A), the middle distance between the substrate and target (B) and near the substrate (C).

Mechanical properties of the prepared coatings were evaluated by nanoindentation using an Ubi1 (Hysitron, Minneapolis) load and depth sensing indentation device. Maximal applied load was varied from 120 μN to 9000 μN on each coating using a commercial diamond Berkovich tip with a tip radius of 806 ± 10 nm, as measured using fused quartz reference material. The load frame compliance of the apparatus and the area function of the Berkovich indenter were also calibrated using the fused quartz standard sample. Hardness and reduced elastic modulus were calculated using the Oliver and Pharr method [7].

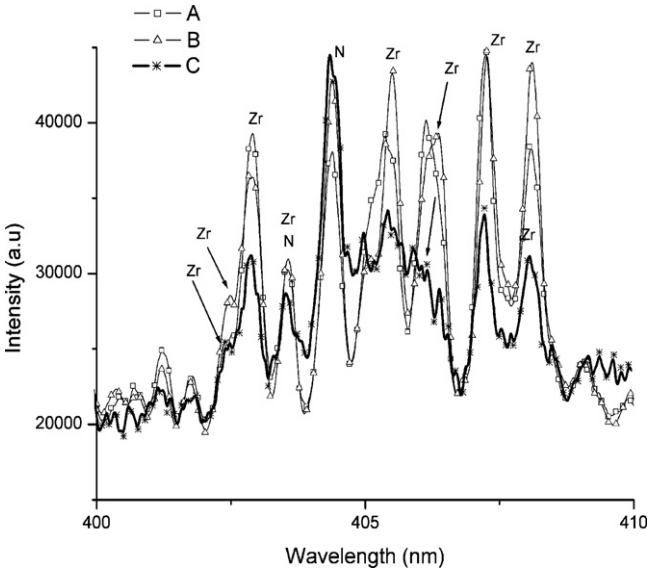

Fig. 2. Emission spectra in the range between 400 nm and 410 nm of wavelength, where emission lines of Zr are clearly identified at different regions of the sputtering plasma.

3. Results and discussion

Emission spectra in different wavelength ranges, where specific atoms or molecules can be identified are shown in Figs. 2–4. In each of these spectra the emission of the different regions of the plasma (A–C) will be compared. For instance, Fig. 2 shows the emission spectra in the wavelength range of 400–410 nm, where the Zr lines can be identified. The different lines corresponding to Zr were identified in all the three regions of the plasma having, however, different intensities. As expected, region A, near the target shows the highest intensity. As mentioned before, the applied deposition technique was RMS, with nitrogen as background gas. The zirconium ions eroded with Argon ions move toward the substrate, finding many nitrogen atoms, reacting to form ZrN molecules, which arrive on the substrate and form a thin film. Thus, the number of Zr ions in the plasma decreases in the direction of the substrate.

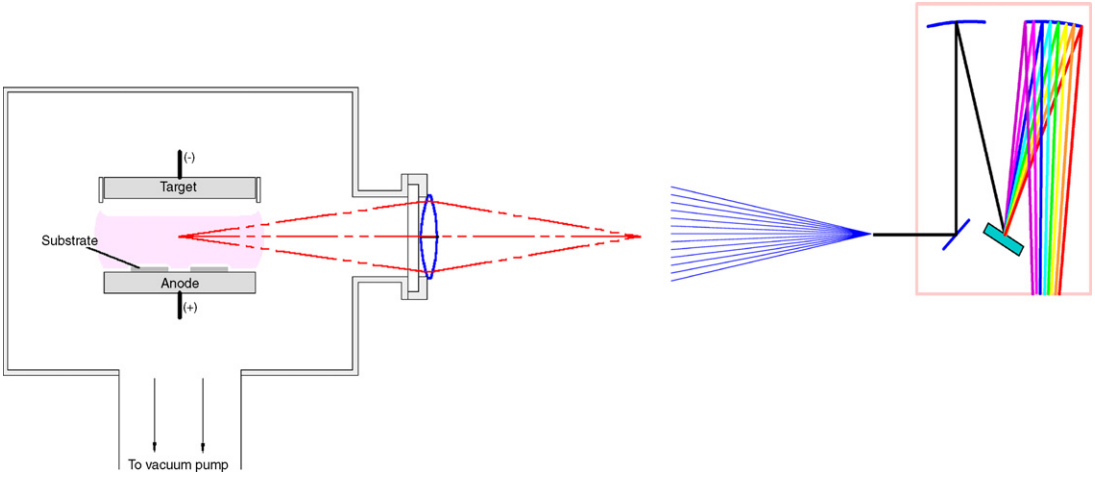

Fig. 1. Schematic representation of the experimental set-up used for optical spectra acquisition.

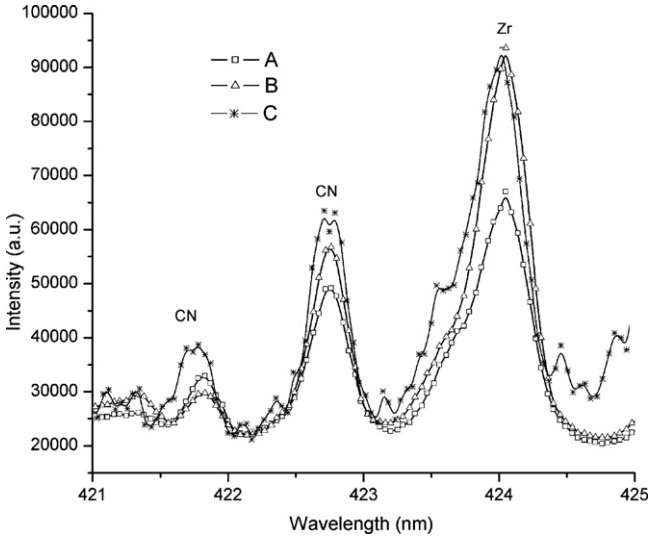

Fig. 3. Emission spectra in the range between 421 nm and 425 nm of wavelength, where CN and Zr emission lines are identified.

This feature is clearly observed in Fig. 2, after a comparison of the intensity of the Zr peaks in the spectra from the different regions of measurement, which diminishes from A to C.

Fig. 3 shows the emission spectra in the wavelength range between 421 nm and 425 nm. In this range, well-known emission lines associated to CN were unambiguously identified. This emission probably corresponds to residual carbon from the chamber walls and steel substrate that reacts with nitrogen leading to CN. Shoonveld reported similar emission lines in the plasma that correspond to CN [11]. From our results, the intensity of these lines shows a slight variation from A to C region (Fig. 3). Note that the shoulder in the 424 nm line is better defined near the substrate. Fig. 5 shows a typical cross-section of the ZrN deposited on SS 316L substrate.

Emission peaks in the plasma associated to chromium were identified in the spectral range 390–400 nm. The presence of Cr in the plasma is probably due to vapor pressure of Cr from the steel substrate, heated at temperatures close 400 °C. In fact, the 394 nm Cr line is much stronger in region C than near the target, which is consistent with this explanation.

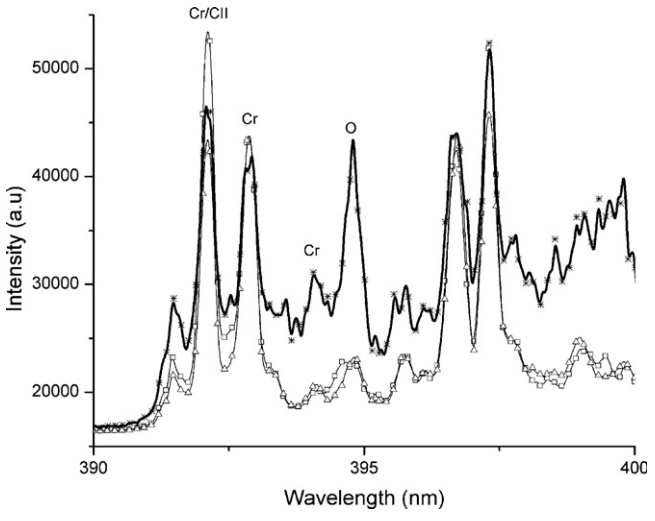

Fig. 4. Emission spectra in the range between 390 nm and 400 nm of wavelength. The emission lines of Cr clearly have higher intensity near the substrate.

The thickness of the film was determined to be around 3 μm (see Fig. 5). The roughness as obtained by AFM measurements was approximately 0.029 μm. Fig. 6 shows a typical X-ray diffraction pattern corresponding to the Zr–N system, which corresponds to a mixture of ZrN and orthorhombic Zr_3N_4 phases. Orthorhombic Zr_3N_4 is a metastable phase, that could be formed when the N_2 partial pressure (or N_2 flux) increases in the chamber [12,13]. Thus, the coexistence of two phases in the film suggest that during the deposition process the N_2 partial pressure reaches a critical level leading to the formation of the Zr_3N_4 phase. The coexistence of the stable and metastable phases has been already reported in the literature [2,13]. A diffraction (2θ) peak at 33.39°, corresponding to a ZrC phase, has been found in these films. The presence of C in the film was confirmed in the Auger depth profile (Fig. 7). The shape of the C peak form in the Auger spectrum is characteristic of carbide compounds. The presence of C in the film may be due to residual gases such as CO_2 or CH_4, which are present as background gases in the vacuum chamber at pressures near to 6.0×10^{-6} Torr. Further on, the optical emission spectra of the plasma shows the presence of CN molecules (Fig. 3) in the three zones of the plasma (A–C). One possibility is that this molecule may be transported through the plasma to the substrate leading to a reaction with the metal. In fact, the C in the Auger signal (see Fig. 7b) could be related to ZrC and CN compounds. The presence of Cr in the plasma is related to the substrate chemical composition, since stainless steel can form a chromium-based oxide protective layer. Thus, during the sputtering process, this protective layer could be removed from the surface. It is important to mention that the Cr was not found in the coating material and this result suggests that Cr is transferred to the plasma.

Other correlation between the Auger depth profile and the plasma diagnostic is the detection of oxygen (Fig. 4). The presence of oxygen is probably attributed either to residual gas in the chamber (CO_2, CH_4, etc.) or to the removal of protective chromium-oxide from the substrate at the beginning of the sputtering process. In fact, the O content is six times higher in the C zone (near substrate) than the A or B zones, which suggests that the O is probably more related to the substrate SS 316L. Finally, the oxygen concentration in the chamber is obviously much lower than that of N_2. However, small oxygen contents can probably lead to formation of a zirconium oxide embedded in the polycrystalline structure of the coating [15].

3.1. Mechanical properties

As mentioned before, the mechanical properties of the coatings were determined by nanoindentation tests in a Hysitron Ubi1 device. Fig. 8 shows typical load–penetration curves obtained at different penetration depths of the prepared ZrN coatings. A penetration depth of 120 nm was probed under the maximal applied load of the nanoindenter (9 mN) (Fig. 8a).

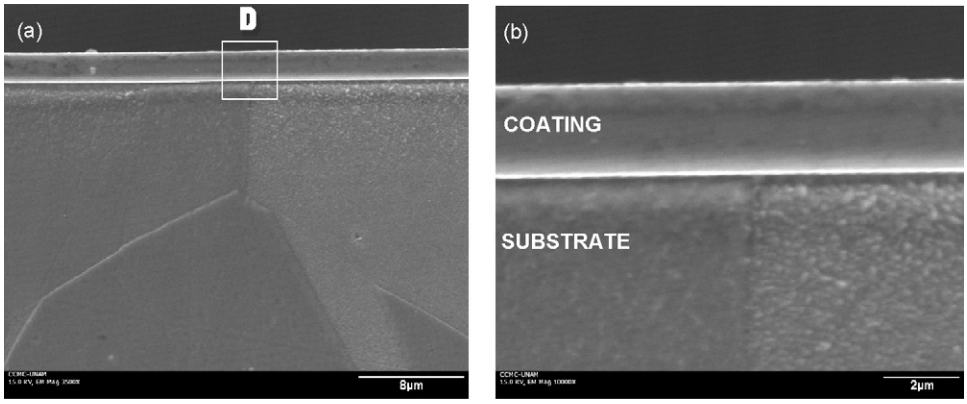

Fig. 5. SEM micrographs showing the cross-section of Zr–N composite on 316L steel.

Considering the variation in stiffness as a function of the applied load, the nanoindentation mean contact pressure beneath the indenter, P_m, was calculated and represented as a function of the ratio of contact to tip radius (a/R) curves (P_m vs. a/R) to describe the different stages of the elastic–plastic behavior of the coatings. These curves clearly show the typical three different regimes as a function of the uniaxial compressive yield stress of the mechanical behavior of the coating. The elastic regime is related to the elastic modulus of the coating, described by the Hertz equation: $P_m = (4E^*/3\pi)a/R$. From this regime, full elastic response was obtained as observed in Fig. 8c and d. Two regions with different slope are observed in the elastic zone. The region of lower penetration depth can probably be associated to a non-homogeneous zirconium oxide thin film, which is commonly formed after the deposition process. According to the experimental load–penetration curves, the thickness of the surface oxide layer is approximately 10 nm. Fig. 8c also shows the relationship between Young modulus and indentation, P_m–a/R curve. The regime of plastic behavior begins at the point marked with z in Fig. 8c, which closely corresponds to an applied load of 3400 μN. At applied loads below 3400 μN no plastic deformation was caused by nanoindentation as measured by AFM in contact mode. At point z of the P_m–a/R curve, the plastic deformation already exists beneath the surface but is constrained by the surrounding elastic material, where the mean contact pressure is higher than the compressive yield stress of

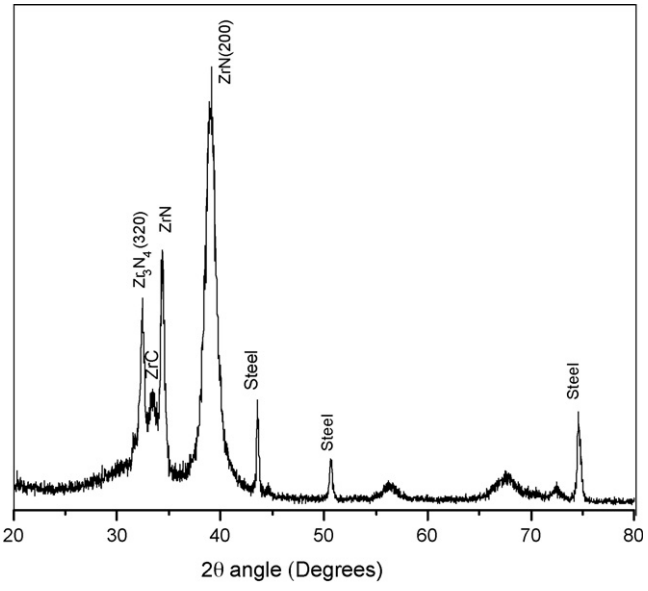

Fig. 6. Typical X-ray diffraction pattern of the prepared coatings.

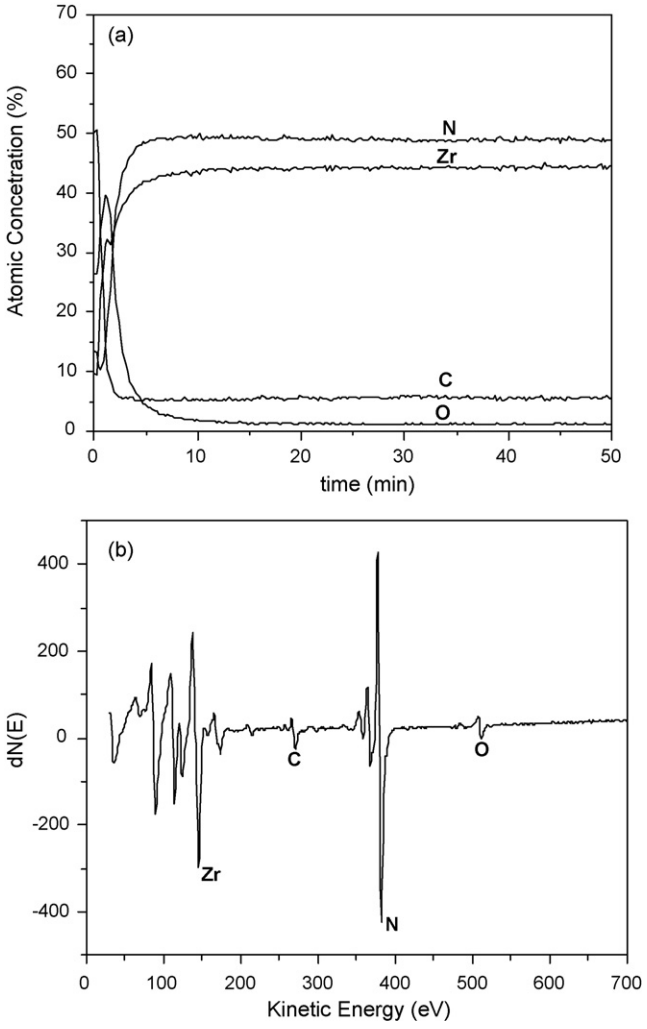

Fig. 7. (a) Auger depth profile for the Zr–N composite and (b) typical Auger spectra Zr–N composite.

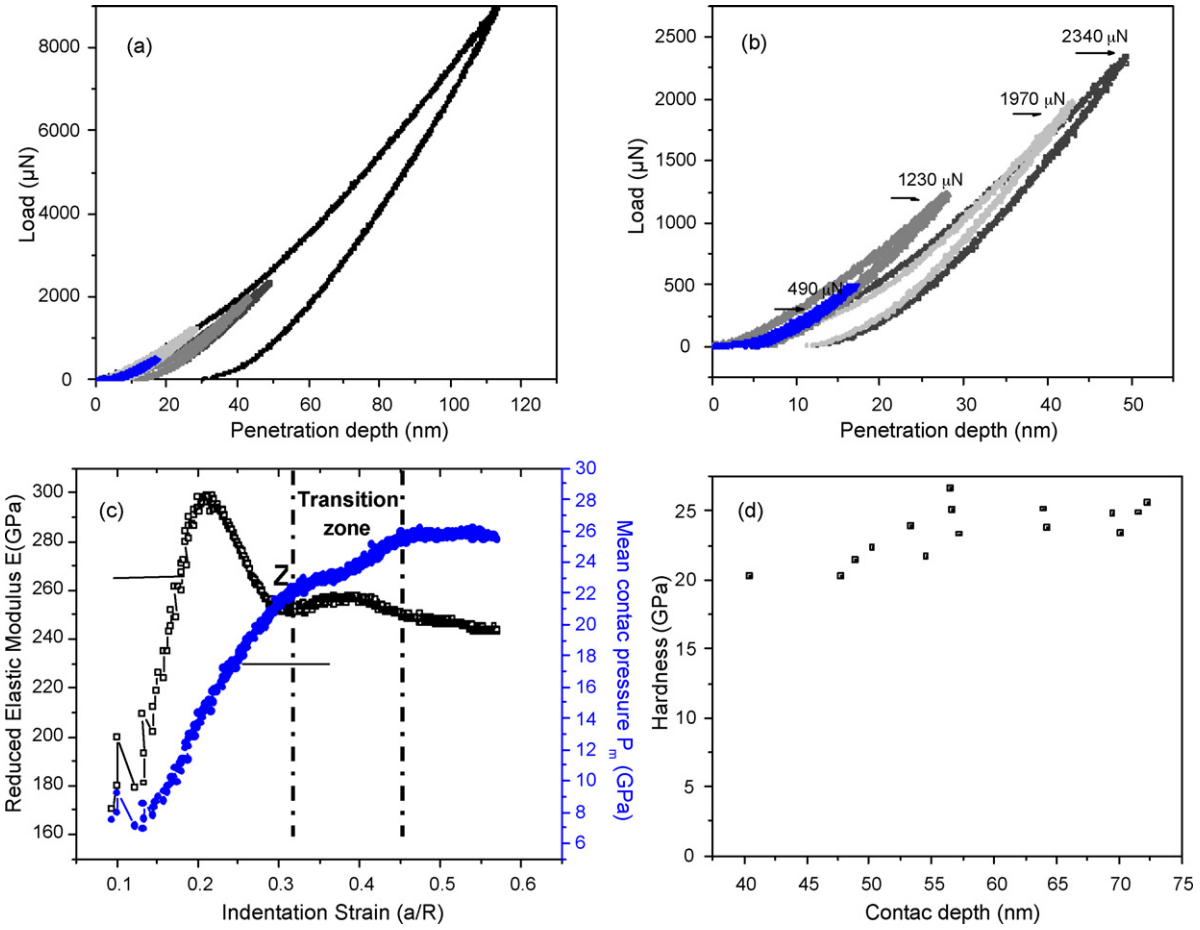

Fig. 8. Results of the mechanical characterization by nanoindentation obtained with a Berkovich indenter. Typical load–penetration curves and at high loads (up to 9 mN) and low loads (max. 2.5 mN) are shown in (a) and (b), respectively. An example of the indentation "stress–strain" curves for the elastic and plastic regimes as well as the hardness dependence with the penetration depth are shown in (c) and (d), respectively.

the material by a factor of 1.1 ($P_m > 1.1\sigma_0$). This factor was obtained by Tabor [14] using the shear stress criteria and the point beneath the indenter, where plastic flow occurs at $\tau = 0.5\sigma_0$.

Finally, the third regime is described with the Tabor relationship ($P_m = C\sigma_0$), which describes the limiting condition of compression, C. In this regime the plastic region extends to the surface of the specimen, where little increase in the mean contact pressure is expected for a homogeneous, continuous and isotropic solid. However, starting from point z, the mean contact pressure shows a transition zone in the range between 0.3 and 0.45 of a/R before it reaches a constant behavior as predicted by the Tabor relationship. This transition zone has a good correlation with the variation of the elastic modulus as a function of a/R in this region. The mentioned transition zone corresponds to penetration depths of the indenter in the range of 25–50 nm.

The hardness of the coating as measured by the Oliver and Pharr method at full applied load was determined to be 25.7 GPa.

It is important to note that the hardness of the coating is not only due to a mixture of ZrN, Zr_3N_4, and ZrC phases. A CN compound in an amorphous phase may also contribute to the mechanical behavior. The values of hardness as a function of penetration depth are shown in Fig. 8d. An almost linear tendency to increase the hardness from 20 to 26 GPa at higher loads is observed. This behavior would support the idea that the CN phase, identified at higher contents on zone C (close to the substrate) contributes to the hardening of the coating. No dramatic influence of the steel substrate at these penetration depths is expected since the thickness of the coatings is much larger than the penetration depth measured at maximal applied load.

Finally, the yield stress of the coating was calculated from these results using the Tabor relationship to be approximately 7.8 ± 0.6 GPa. The Young's modulus of the coating was obtained with data from the deeper region in the elastic zone from the plastic zone, to avoid the influence of the zirconium oxide thin film. This value was calculated using the (a/t) factor where a is the radius of the contact area and T is the coating thickness. Then Young's modulus is determined by the extrapolated value at $a/t = 0$. So the Young modulus is about 380 GPa.

Thus, the characterization of the sputtering plasma in different regions seems to be an excellent tool to explain gradients in physical and mechanical properties, and determine the deposition conditions that may render the optimal mechanical properties of the coating. The present study reveals

components of the plasma directly correlated with the mechanical properties of the coating. In particular, the detection of CN molecules in the plasma that allows the understanding of the improvement in mechanical behavior of the coating as a function of penetration depth.

4. Conclusions

Unbalanced reactive magnetron sputtering using a Zr target on stainless steel produces multiphase coatings due to the reaction of the nitrogen gas with the target and the substrate. Characterization of plasma allowed the understanding of the mechanical properties of the coatings. For instance, the presence of CN molecules in the prepared coatings was identified by optical spectroscopy. It was observed that the intensity corresponding to emissions from CN molecules, increased in the plasma region from the target to the substrate. Also ZrN, Zr_3N_4 and ZrC phases coexist in the coating. There is a tendency of the hardness to increase at higher penetration depth from 20 GPa to 26 GPa. This behavior can be due the presence of CN molecules formed during the deposition process and determined by optical spectroscopy in the plasma, with higher concentrations in regions close to the substrate. The CN molecule seems to play an important role in explaining the increasing tendency of the hardness as a function of the indentation penetration depth.

Acknowledgements

This work has been financed by CONACyT projects: 47714-F, 44850 and 42568-Q. The authors like to thank gratefully the support given by E. Flores Aquino, E. Aparicio and M. Sainz of CCMC-UNAM and J. Davalos of CICESE.

References

[1] S. Camelio, T. Girardeau, L. Pichon, A. Straboni, C. Fayoux, Ph. Guerin, J. Opt. A: Pure Appl. Opt. 2 (2000) 442.
[2] L. Pichon, T. Girardeau, A. Straboni, F. Lignou, P. Guerin, J. Perriere, Appl. Surf. Sci. 150 (1999) 115.
[3] D. Pilloud, A.S. Dehlinger, J.F. Pierson, A. Roman, L. Pichon, Surf. Coat. Technol. 174/175 (2003) 338.
[4] G. Lopez, M.H. Staia, Surf. Coat. Technol. 200 (2005) 2092.
[5] D. Wu, Z. Zhang, W. Fu, X. Fan, H. Guo, Appl. Phys. A 64 (1997) 593.
[6] C.R. Liu, H.G. Yang, Thin Solid Films 444 (2003) 111.
[7] W.C. Oliver, G.M. Pharr, J. Mater. Res. 7 (1992) 1564.
[8] E. Pérez-Tijerina, J. Bohigas, R. Machorro, Rev. Mex. Fís. 51 (153) (2005).
[9] E. Pérez-Tijerina, J. Bohigas, R. Machorro, J. Appl. Phys. 90 (2001) 3192.
[10] E. Pérez-Tijerina, R. Machorro, J. Bohigas, Rev. Sci. Instrum. 75 (2004) 455.
[11] L.H. Shoonveld, J. Chem. Phys. 58 (1973) 403.
[12] T. Yotsuya, M. Yoshitake, T. Kodamat, Cryogenics 37 (1997) 817.
[13] Z. Zhiguo, L. Tianwei, X. Jun, D.X. Lu, D. Chuang, Surf. Coat. Technol. 200 (2006) 4998.
[14] D. Tabor, Hardness of Metals, Clarendon Press, Oxford, 1951.
[15] L. Cunha, F. Vaz, C. Moura, L. Rebouta, P. Carvalho, E. Alves, A. Cavaleiro, Ph. Godeau, J.P. Riviere, Surf. Coat. Technol. 200 (2006) 2917.